Carbon – Science and Technology

ISSN 0974 – 0546

http://www.applied-science-innovations.com

ARTICLE Received : 13/05/2013, Accepted : 15/08/2013

Special Section on Advanced (Non-Carbon) Materials

Ferromagnetic Ni-doped ZnO nanoparticles synthesized by a chemical precursor method

Jeevan Jadhav [#], Mahesh Patange [#], and Somnath Biswas [*]

Department of Physics, The LNM Institute of Information Technology, Jaipur-302031, Rajasthan, India.

[#] Contributed equally; ***Corresponding Author**, Tel : +91-7597171575; Fax : +91-141-5189214.

A simple chemical synthesis method of pristine ZnO and Ni-doped ZnO ($Ni_xZn_{1-x}O$; x = 0.01-0.05) nanoparticles is reported. Structural and morphological properties of the synthesized nanoparticles have been studied using X-ray diffraction (XRD), Fourier transform infrared spectroscopy (FTIR), vibrating sample magnetometer (VSM), and high-resolution transmission electron microscopy (HRTEM). Average crystallite size calculated from XRD peak widths using Debye Scherrer's formula comes out to be 12 nm, 8 nm and 10 nm in pristine ZnO, $Ni_{0.01}Zn_{0.99}O$, and $Ni_{0.05}Zn_{0.95}O$ samples, respectively. HRTEM images clearly show high crystalline order in the derived nanoparticles with particle size of 15-18 nm, which are in good agreement with the XRD results. Magnetic measurements reveal that the incorporation of Ni^{2+} cations into the ZnO lattice results in induced room-temperature ferromagnetism in the otherwise non-magnetic ZnO.

Keywords : ZnO, Ni-doped ZnO, Diluted magnetic semiconductors, Ferromagnetism.

1. Introduction : ZnO is an attractive wide band gap II-VI semiconductor for potential applications in various fields including optical transducers, UV light emitters, transparent solar cells, electrochemical coupled sensors, and spintronic devices **[1 - 6].** Recently, much research attention is focused on ZnO nanocrystals or quantum dots due to their striking optical properties owing to the quantum confinement effects **[7 - 9].** The large excitation binding energy (~60 meV) makes it an excellent phosphor material for UV light emitting diodes.

In recent years, there has been a significant interest towards the use of the additional degree of spin of electrons besides its charge for novel applications. Ferromagnetic functionality induced in transition metal (TM) ion doped ZnO further extends its potentiality for novel spintronics applications. Dietl *et al.*, first reported a theoretical model to explain the observed ferromagnetism in TM doped wide band gap diluted magnetic semiconductors (DMS) **[10].** Proper choice of the doping materials into the semiconductors can tailor potential electrical, optical and magnetic properties, which can have significant effects in the performance of DMS based devices. In this regard, ZnO based DMS materials with high Curie temperature (T_C) are being considered as one of the most promising materials for spintronics devices. In literature, there are several reports on the properties of TM (e.g. Mn, Fe, Co, Ni) doped ZnO materials. The results show that the induced magnetization is very sensitive to the nature of doping, doping concentration and the synthesis techniques **[1, 2].**

Amongst the several transition metal doped ZnO DMS materials, Ni-doped ZnO nanoparticles are favorable for potential applications due to its comparatively high T_C value.

Here, we report a novel synthesis method of pristine ZnO and Ni-doped ZnO ($Ni_xZn_{1-x}O$) nanoparticles via a polymer precursor. The structural and magnetic properties of the as-synthesized nanoparticles were studied in details.

2. Experimental :

Materials : The materials used in the synthesis process were zinc nitrate hexahydrate [mol. wt. = 297.47, 99.98 % pure], nickel nitrate hexahydrate [mol. wt. = 290.81, 99.95 % pure], *poly*-vinyl alcohol (PVA) [mol. wt. ~50000, degree of polymerization ~1800], 25 % ammonia solution, sucrose (99 % pure). Zinc nitrate hexahydrate and nickel nitrate hexahydrate were procured from Sigma Aldrich. PVA and sucrose were purchased from Fisher Scientific and used without further purifications.

Synthesis and Methods :

2.1 Preparation of a polymer precursor : The basic idea behind the synthesis technique is to control the growth of the nanoparticles in the reaction solution by encapsulating in polymer micelles **[11].** For synthesizing the pristine ZnO nanoparticles, aqueous solution of Zn^{2+} ions was slowly added in freshly prepared aqueous solution of PVA-sucrose under constant stirring at 60 - 65 °C. After aging the reaction solution at 24 h, the final precipitate was washed with methanol to remove excess PVA-sucrose and dried at a controlled temperature of 50-60 °C to get a polymer capped ZnO precursor powder.

The Ni-doped ZnO nanoparticles were synthesized by dispersing aqueous solutions of Ni^{2+} and Zn^{2+} in PVA-sucrose solution. With the addition of metal (Ni^{2+} and Zn^{2+}) salt solutions in the basic PVA-sucrose solution, metal ions were trapped in the polymer micelles in the form of metal hydroxides. PVA is a good reducing as well as a capping agent thereby enhances the reductive oxidation of salts of the metals. The reactions involved are

$$(Zn^{2+} + NO_3^{2-}) + 2(NH_4^+ + OH^-) + PVA \rightarrow Zn(OH)_2 + PVA + 2NH_3\uparrow + HNO_3$$

$$(Ni^{2+} + NO_3^{2-}) + 2(NH_4^+ + OH^-) + PVA \rightarrow Ni(OH)_2 + PVA + 2NH_3\uparrow + HNO_3.$$

The metal hydroxide precipitates were soluble in basic medium producing the metal oxide anions (zincates/nickelates) which were trapped in the polymer micelles and after the aging nucleate to produce the stable size controlled metal oxide nanoparticles.

$$Zn(OH)_2 + (NH_4^+ + OH^-) \rightarrow ZnO_2^{2-} + NH_3\uparrow + H_2O$$

$$Zn(OH)_2 + Ni(OH)_2 + (NH_4^+ + OH^-) \rightarrow Ni_xZn_{1-x}O_2^{2-} + NH_3\uparrow + H_2O.$$

The precursor powders were calcined at 400-600°C to get the recrystallized pristine and Ni doped ZnO nanoparticles.

2.2 Physico-chemical Characterization

2.2.1 X-ray Diffraction (XRD) Analysis : The crystalline nature of the as-synthesized nanoparticles were analyzed with an X-ray diffractometer of Panalytical`s *X`Pert Pro* using CuK_α radiation of 0.1545 nm.

2.2.2 High Resolution Transmission Electron Microscopy (HRTEM) Analysis : JEOL-2100 HRTEM was used to study the microstructural features in the derived samples.

2.2.3 Fourier Transform Infrared (FTIR) Analysis : The FTIR spectra of the precursors and calcined samples were recorded at room temperature using Perkin Elmer PE 1600 spectrometer.

2.2.4 VSM Analysis : Magnetic hysteresis loop (M-H curve) of the derived samples were recorded at room temperature using a Lake Shore VSM with a maximum field of 15 k Oe.

3. Results and Discussion :

3.1 Structural Analysis : Figure (1) shows the X-ray diffraction patterns of pristine and Ni-doped ZnO samples calcined at 400°C for 2 h in ambient air. The samples show distinctive peaks of hexagonal wurtzite type crystal lattice (JCPDS card no. 36-1451). No peaks of Ni and NiO are

observed in the XRD pattern. Thus, Ni^{2+} ions do not form precipitates during the doping reaction but selectively replace the Zn^{2+} positions in the ZnO crystal lattice. The average crystallite size calculated from full width half maxima (FWHM) values of the diffraction peaks and the Debye Scherrer`s formula comes out to be 12 nm, 8 nm and 10 nm, respectively, for pristine ZnO, $Ni_{0.01}Zn_{0.99}O$ and $Ni_{0.05}Zn_{0.95}O$ nanoparticles. The lattice parameters in the samples are given in Table (1).

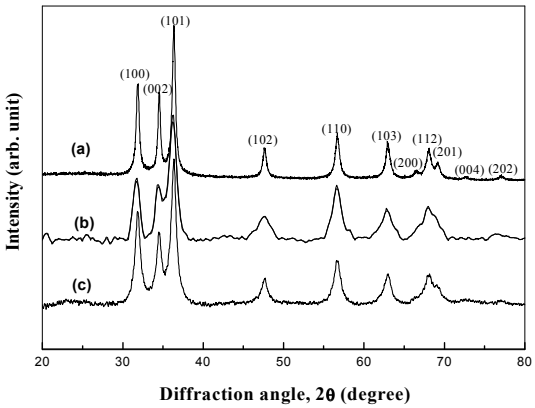

Figure (1) : X-ray diffraction in (a) ZnO nanoparticles after heating a Zn^{2+}-PVA-sucrose precursor powder at 400°C for 2 h, and (b) $Ni_{0.01}Zn_{0.99}O$ and (c) $Ni_{0.05}Zn_{0.95}O$ nanoparticles after heating the respective Zn^{2+}-Ni^{2+}-PVA-sucrose precursor powders at 400°C for 2 h in ambient air.

Table (1) : Average crystallite size and lattice constants of pristine and doped ZnO samples calcined at 400 °C.

	Average crystallite size (nm)	Lattice constants (nm)
Pristine ZnO	12	$a = 0.3254$ $c = 0.5220$
$Ni_{0.01}Zn_{0.99}O$	8	$a = 0.3262$ $c = 0.5232$
$Ni_{0.05}Zn_{0.95}O$	10	$a = 0.3255$ $c = 0.5215$

3.2. FTIR Analysis : Figure (2) shows the FTIR spectra of pristine and Ni-doped ZnO samples calcined at 400°C in ambient air. All the distinct bands observed in the samples are listed in Table (2). The observed bands at 430-660cm^{-1} in the pristine ZnO as well as Ni-doped ZnO samples have been assigned to the Zn-O stretching vibrations in the hexagonal wurtzite type crystal structure.

Table (2) : The observed FTIR bands in the pristine and Ni-doped ZnO samples calcined at 400°C.

Bands	Pristine ZnO	$Ni_{0.01}Zn_{0.99}O$	$Ni_{0.05}Zn_{0.95}O$	Ref.
Zn-O stretching	430-650 cm^{-1}	450-660 cm^{-1}	451-660 cm^{-1}	[4]
NO_3^{2-} stretching	846 cm^{-1}	840 cm^{-1}	820 cm^{-1}	[12]
Polymeric bending vibration stretches	1590 cm^{-1} (Broad band)	1640 cm^{-1} (Broad band)	1635 cm^{-1} (within broad band)	[3]
M (metal)-CO stretching	2208 cm^{-1}, 2340 cm^{-1}	2219 cm^{-1}, 2350 cm^{-1}	2219 cm^{-1}	[3,12]
O-H stretching	3360 cm^{-1}	3350 cm^{-1}, 3600 cm^{-1}	3368 cm^{-1}	[4,12]

The adsorption of CO at room temperature produces overtone bands around 2200 cm^{-1} region **[3, 12];** therefore, the sharp bands at 2219 cm^{-1} and 2350 cm^{-1} can be correlated to overtone bands from M-CO stretching (where, M-transition metal). The frequency of the absorption bands for the M-CO stretching not only depends on the charge balancing metal cations but also upon the composition framework **[12].** In the pristine and $Ni_{0.01}Zn_{0.99}O$ samples, the two M-CO overtone bands (around 2219 cm^{-1} and 2350 cm^{-1}) are observed while that in $Ni_{0.05}Zn_{0.95}O$ samples only one band at 2219 cm^{-1} is observed. The other bands at 1650 cm^{-1} and the broad band at 3350 cm^{-1} are assigned to the bending vibrations of the polymeric matrix and the stretching vibration of the hydroxyl group, respectively.

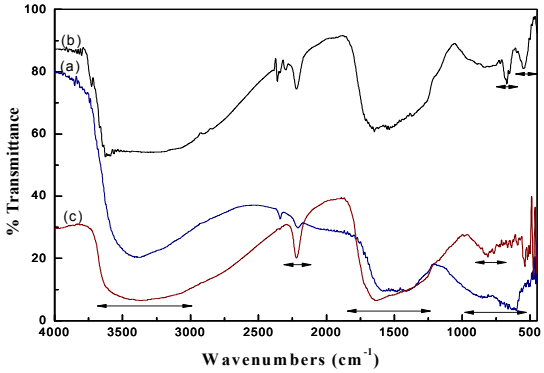

Figure (2) : FTIR spectra of (a) pristine ZnO, (b) $Ni_{0.01}Zn_{0.99}O$, and (c) $Ni_{0.05}Zn_{0.95}O$ samples calcined at 400°C for 2 h in ambient air.

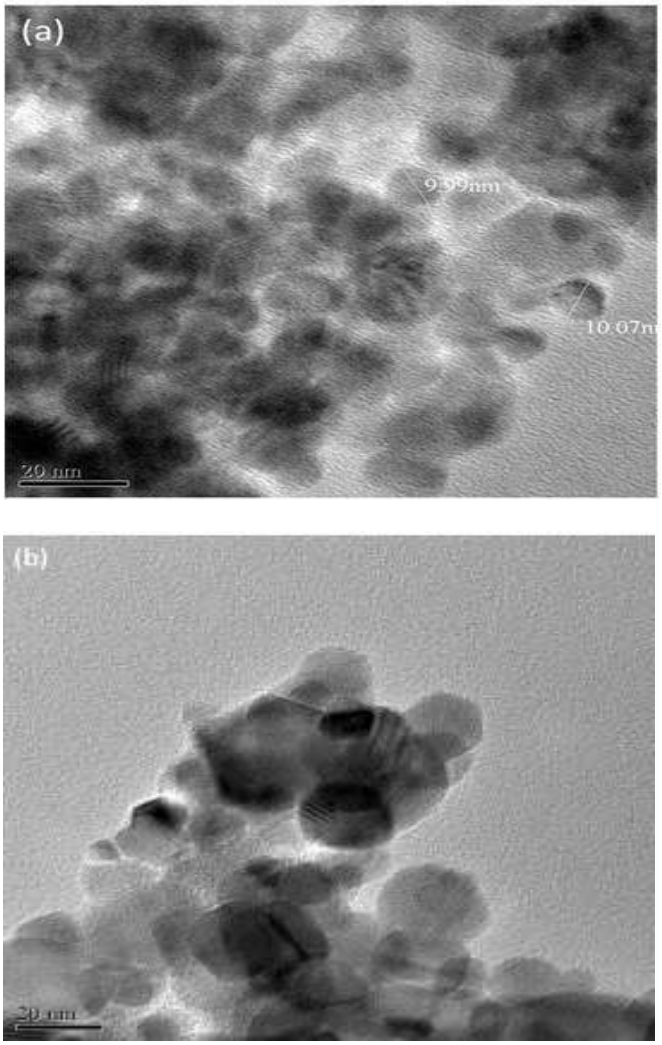

Figure (3) : TEM micrographs of (a) pristine ZnO and (b) $Ni_{0.05}Zn_{0.95}O$ nanoparticles calcined at 400 °C for 2 h in ambient air.

3.3. HRTEM Analysis : Figure (3) shows typical HRTEM micrographs of the pristine and $Ni_{0.05}Zn_{0.95}O$ nanoparticles. The images clearly show well dispersed nanoparticles of average size ~12 nm and 16 nm in the pristine and $Ni_{0.05}Zn_{0.95}O$ nanoparticles calcined at 400 °C. The observed particle sizes matches well with the XRD results.

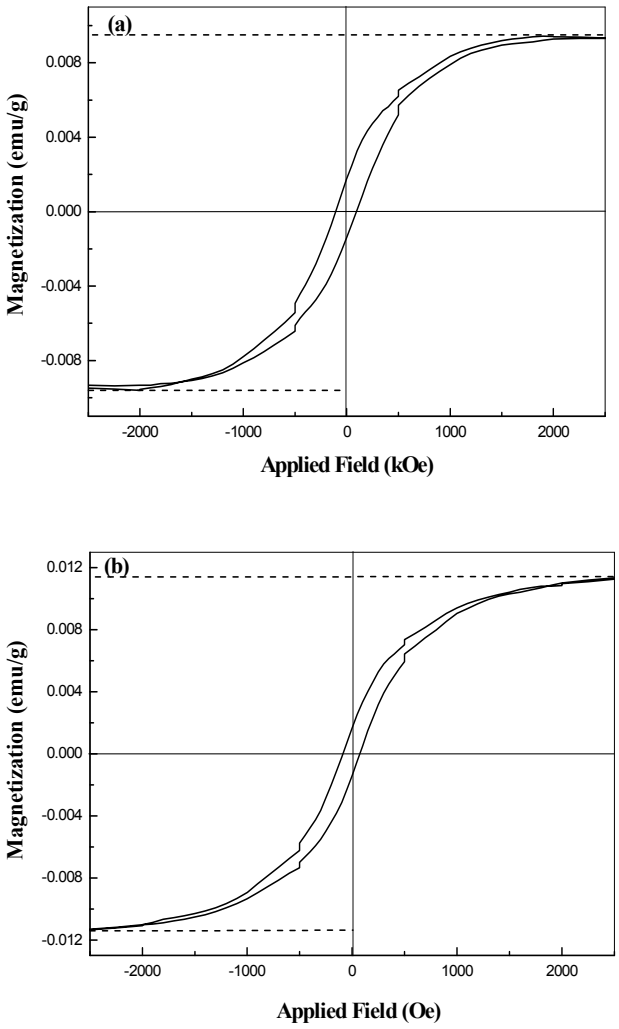

Figure (4) : Room temperature magnetic hysteresis loop of $Ni_{0.01}Zn_{0.99}O$ nanoparticles calcined at (a) 400 °C and (b) 500 °C for 2 h in ambient air.

3.4. VSM Analysis : The ferromagnetic properties of the Ni-doped ZnO samples were measured with VSM at room temperature and the results are shown in Figure (4). The ferromagnetic ordering in the ZnO based DMS materials is carrier mediated ferromagnetism **[2],** which

depends on the type and carrier density of the magnetic dopants. The magnetic properties measured in 1% Ni-doped ZnO samples are given in Table (3). It is observed that the resultant coercivity value decreases with the increase in the annealing temperature.

Table (3) : Magnetic properties of $Ni_{0.01}Zn_{0.99}O$ samples

	$Ni_{0.01}Zn_{0.99}O$ calcined at 400°C	**$Ni_{0.01}Zn_{0.99}O$ calcined at 500°C**
Coercivity	93 Oe	74 Oe
Saturation Magnetization	9.47×10^{-3} emu/g	11.20×10^{-3} emu/g
Remanent Magnetization	1.14×10^{-3} emu/g	1.48×10^{-3} emu/g
Percentage Remanence	~12 %	~13 %

In literature, either the super-exchange and double-exchange interactions between the *d*-states of doped Ni^{2+}-Ni^{2+} magnetic ions, or free-carrier mediated exchange or *sp-d* exchange interactions between host ions and magnetic ions are reported to be responsible for producing this type of room temperature ferromagnetism in Ni-doped ZnO nanocrystals **[13, 14].**

4. Conclusions : In conclusion, pristine and Ni-doped ZnO nanoparticles of controlled size have been synthesized by a novel chemical synthesis method. HRTEM images show homogeneous nanocrystals with an average particle size of 12 nm and 16 nm in the pristine and $Ni_{0.05}Zn_{0.95}O$ samples, respectively, which are in good agreement with XRD results. The observed magnetic hysteresis loop in the Ni-doped samples confirms induced ferromagnetism in the as-synthesized Ni-doped ZnO samples.

Acknowledgments : The authors sincerely thank (i) Sophisticated Analytical Instrument Facility (SAIF), North-East Hill University (NEHU), Shillong, (ii) Department of Physics, University of Pune and (iii) S. C. S. College, Omerga for providing us the instrumental facilities.

References :

[1] C. J. Cong, J. H. Hong, Q. U. Liu, L. Liao, K. L. Zhang, Synthesis, structure and ferromagnetic properties of Ni-doped ZnO nanoparticles, Solid State Comm. 138(10-11) (2006) 511 - 515.

[2] G. J. Huang, J. B. Wang, X. L. Zhong, G. C. Zhou, H. L. Yan, Synthesis, structure and room temperature ferromagnetic properties of Ni-doped ZnO nanoparticles, J. Mater. Sci. 42 (2007) 6464 - 6468.

[3] P. R. Patil, S. S. Joshi, Polymerized organic-inorganic synthesis of nanocrystalline zinc oxide, Mater. Chem. Phys., 105/2-3 (2007) 354 - 361.

[4] D. M. Fernendes, A. A. Winkler Hechenleitner, M. F. Silva, M. K. Lima, P. R. Stival Bittencourt, R. Silva, M. A. Custogdio MeLo, E. A. Gomez Pineda, Preparation and characterization of NiO, Fe_2O_3, $Ni_{0.04}$ $Zn_{0.96}O$ and $Fe_{0.03}$ $Zn_{0.97}O$ nanoparticles, Mater. Chem. Phys. 118/2-3 (2009) 447 - 452.

[5] R. Chauhan, A. Kumar, R. Chaudhary, Structure and optical properties of $Zn_{1-x}Ni_xO$ nanoparticles by coprecipitation method, J. Optoelectron. Biomed. Mater. 3/1 (2011) 17 - 23.

[6] K. Srinivas, S. M. Rao, P. V. Reddy, Preparation and properties of $Zn_{0.9}Ni_{0.1}O$ diluted magnetic semiconductor nanoparticles, J. Nanopart. Res. 3/2 (2011) 817 - 837.

[7] D. A. Schwartz, N. S. Norberg, Q. P. Nguyen, J. M. Parker, D. R. Gamelin, Magnetic quantum dots: synthesis, spectroscopy, and magnetism of Co^{2+}- and Ni^{2+}-doped ZnO nanocrystals, J. Am. Chem. Soc. 125 (2003) 13205 - 13218.

[8] K-F. Lin, H-M. Cheng, H-C. Hsu, L-J. Lin, W-F. Hsieh, Band gap variation of size-controlled ZnO quantum dots synthesized by sol-gel method, Chem. Phys. Lett. 409/4-6 (2005) 208 - 211.

[9] B. B. Li, X. Q. Xiu, R. Zhang, Z. K. Tao, L. Chen, Z. L. Xie, D. Zheng, X. Xie, Study of structure and magnetic properties of Ni-Doped ZnO-based DMSs, Mater. Sci. Semicon. Proc. 9 (2006) 141 - 145.

[10] T. Dietl, H. Ohno, F. Matsukura, J. Cibert, D. Ferrand, Zener model description of ferromagnetism in zinc-blend magnetic semiconductors, Science 287 (2000) 1019 - 1022.

[11] S. Biswas, S. Ram, Morphology and stability in a half-metallic ferromagnetic CrO_2 compound of nanoparticles synthesized via a polymer precursor, Chem. Phys. 306/1-3 (2004) 163 - 169.

[12] V. Rakic, V. Dondur, R. Hercigonja, FTIR study of carbon monoxide adsorption on ion-exchanged X, Y and mordenite type zeolietes, J. Serb. Chem. Soc. 68 (2003) 409 - 4016.

[13] P. V. Radovanoic, D. R. Gamelin, High-temperature ferromagnetism in Ni^{2+} doped ZnO aggregates prepared from colloidal diluted magnetic semiconductor quantum dots, Phys. Rev. Lett. 91/15 (2003) 157202 (1 - 4).

[14] J. Iqbal, B. Wang, X. Liu, D. Yu, B. He, R. Yu, Oxygen-vacancy-induced green emission and room-temperature ferromagnetism in Ni-doped ZnO nanorods, New J. Phys. 11/6 (2009) 063009.